"Synthesis of Lead Chalcogenides Nanocubes at Room Temperature by Solution Chemical Method"

A dissertation submitted towards the partial fulfillment of
the requirement for the award of degree of

Master of Technology
in
Nano Science and Technology

Submitted by

Rajeev Verma
2K13/NST/12

Under the supervision of

Dr. Amrish K. Panwar
(Assistant Professor, Department of Applied Physics)

Delhi Technological University
(Formerly Delhi College of Engineering)
Bawana Road, Delhi-110042
July 2015

Delhi Technological University
Department of Applied Physics
Bawana Road, Delhi-42

CERTIFICATE

This is to certify that work which is being presented in the dissertation entitled **"Synthesis of Lead Chalcogenides Nanocubes at Room Temperature by Solution Chemical Method"** is the authentic work of **Rajeev Verma (2K13/NST/12)** under my guidance and supervision in the partial fulfillment of requirement towards the degree of **Master of Technology** in **Nano Science and Technology**, run by Department of Applied Physics in Delhi Technological University during the year 2013-2015. As per the candidate declaration the research work reported and the results presented in this thesis have not been submitted in parts or in full to any other University or Institute for the award of any other degree.

Dr. Amrish K. Panwar
Supervisor
Asst. Professor, Dept. of Applied Physics
Delhi Technological University
Delhi

Prof. S. C. Sharma
H.O.D., Applied Physics
Delhi Technological University
Delhi

DECLARATION

I, hereby, declare that all the information in this document has been obtained and presented in accordance with academic rules and ethical conduct. This report is my own, unaided work. I have fully cited and referenced all material and results that are not original to this work. It is being submitted for the degree of Master of Technology in Nano Science and Technology at the Delhi Technological University. It has not been submitted before for any degree or examination in any other university.

Signature :
Name: Rajeev Verma
Roll no. 2K13/NST/12

ACKNOWLEDGEMENT

I take this opportunity as a privilege to thank all individuals without whose support and guidance I could not have completed my project successfully in this stipulated period of time.

First and foremost I would like to express my deepest gratitude to my supervisor **Dr. Amrish K. Panwar**, Asst. Professor, Department of Applied Physics, Delhi Technological University for his invaluable support, guidance, motivation and encouragement throughout the period this work was carried out.

I would also like to express my indebtedness to **Prof. S.C. Sharma**, HOD, Applied Physics, Delhi Technological University, for providing all kinds of help required through the department.

I would like to express my sincere thanks to my M.Tech coordinator**, Dr.P.K.Tyagi**, Assistant Professor, Department of Applied Physics, Delhi Technological University.

I am also thankful to **Mr Rakesh Saroha** and **Mr. Aditya Jain (Research scholars)** for their valuable support and guidance in carrying out this project.

I would also like to thank to all my friends and colleagues who have patiently extended all sorts of help for accomplishing this work.

Above all, I am indebted to the Almighty for blessing me with potential to carry out the project besides my parents for encouraging me during the completion of the dissertation

Rajeev Verma
2k13/NST/12

Abstract

Energy crisis and thermal management related issues have been highlighted in the modern century due to escalating demands for energy consumption and global warming from fossil fuels. Sustainable and alternative energy sources are ever growing global concern. Thermoelectric (TE) materials have gained significant interest, due to effective solid-state energy conversion from waste heat to useful electrical energy and vice versa. Clean, noise-free, and environment-friendly operation of TE devices has triggered great attention in viable technologies including automotive, military equipment, aerospace, and industries to scavenge waste heat into power. Till date conventional TE materials have shown limited energy conversion efficiency in the form of thermoelectric Figure of Merit (*ZT*). However, the concept of nanostructure and development of novel TE materials have opened excellent way to improve significant values of *ZT*. Nano-engineered bulk TE materials allow effective phonon scattering at the high density of grain boundaries, which offer a way of lowering the thermal conductivity.

Mass-scale synthesis of TE nanomaterials is a challenge for the TE industry because of expensive fabrication processes involved. This study reports a bottom-up chemical synthesis route performed at room temperature and can be utilized to produce highly pure, homogenous and highly crystalline TE lead chalcogenides nanoparticles of PbSe and PbTe. XRD patterns observed for synthesized powder confirm the pure phase of PbSe and PbTe. Cubic shape nanoparticles of PbSe and PbTe are synthesized successfully at room temperature as observed by scanning electron microscope images. The size of particles was calculated from high intense peak of XRD pattern using Debye Scherrer formula. Hence uniformly distributed regular cube particle of size 28.49 nm of PbSe and 30.975 nm for PbTe are observed.

Keywords*:* Thermoelectric, Figure of merit, Nano-engineering, Chalcogenides.

List of Abbreviations and Symbols

COP	Coefficient of performance
DOS	Density of states
PGEC	Phonon glass electron crystal
XRD	X-Ray diffraction
SEM	Scanning electron microscope
EDS	Energy dispersive X-ray spectroscopy
TE	Thermoelectric
emf	Electro motive force
mfp	Mean free path
S	Seebeck coefficient
$S^2\sigma$	Power factor
ZT	Thermoelectric figure of merit
σ	Electrical conductivity
P	Electrical resistivity
κ	Thermal conductivity
κ_e	Electronic thermal conductivity
κ_l	Lattice thermal conductivity
Π	Peltier coefficient
μ	Thomson coefficient, charge mobility
J	Current density
m^*	Effective mass
L	Lorenz number

List of figures

Table of Contents

Chapter 1

Introduction

The world is currently facing energy crisis because of increasing demand of power globally. On the other hand, there is a persistent worry about the impact of greenhouse gasses (GHGs), particularly CO_2, on the earth. These issues are driving the interest for generating green energy and acquiring more useful energy use. Research and developments is in progress to provide a way for efficient use of energy. For example, newly designed engines, transmissions and related advancements are work in progress to expand transport vehicle fuel productivity. However, these innovations are missing critical issue: The waste heat. We are dependent on conventional sources (fossil fuels, nuclear fuels) and non-conventional sources (solar energy, wind energy, tidal energy) to meet our power demands. All power generation methods involve very less efficiency and a lot of energy is wasted in form of heat. Similarly during consumption of power, our machines produce a lot of heat because of insufficiency in conversion of energy into useful work. Effective harvesting of this waste heat can improve power generation efficiency and power utilization efficiency; this way can help in order to meet our increasing power demand.

In addition to power generation, effective heat management solves numerous other problems. For example semiconductor based electronic devices start performing poorly when they are operated at higher temperature for long time because properties of semiconductor materials are temperature dependent. Due to advancement in VLSI (very large scale integration) and ULSI (ultra large scale integration) technology the size of IC (integrated circuits) is reduced but resulted in increased heat generation in chips up to 100 W/cm^2 [1]. Bar-Cohen et al. demonstrated that the durability of the IC is decreased by 10% for each rise of 2˚C in temperature [2]. A research unit of U.S. Air Force claimed that almost half of the total malfunctioning in electronics devices is because of temperature related problems [3]. So excessively generated heat has become a limiting factor for further reduction in size of CMOS based IC and that's why Moore's law does not hold well anymore. Therefore it is inevitable that management of enormously generated heat and design of logic should be considered concurrently for further developments in electronics world. [4].

Thermoelectric technique provides such an opportunity to convert waste heat into useful electrical energy as well as to cool ambience and is ecofriendly in nature. This technique is being used in cooling diode lasers, portable refrigeration, cool/ heat car seats. Thermoelectric cooling is also used in infrared imaging based sensors which require a very low temperature ($-80^{\circ}C$).These sensors are used in night vision equipment and heat guiding missile system [5]. In other ways, this technique is being used for thermoelectric power generation because of its reliability, nature friendly operations because during operation harmful gases like CFCs, CO_2 are not liberated and maintenance cost of operation is also very low. These power generators are very useful when the durability with longer operating life under extreme conditions are required. Silicon and germanium are used as high temperature power generation materials. Advantage of these materials is that they enable production of heat engines without any mechanical part. So they are very reliable for space application and can function even in absence of the solar energy. Generally the solar cells are used for power generation in spacecraft but they require adequate solar radiant flux which is available up to planet Mars. For space mission program beyond the Mars, thermoelectric provide an alternative for power generation. Thermoelectric heat engines are successfully used by all deep-space missions launched by US and former USSR [6,7]. Micro-thermoelectric generators are being successfully used in many low power devices such as hearing aids and wrist watches launched by Seiko and Citizen [7].

Various thermoelectric materials like Bi_2Te_3, lead chalcogenides, Si-Ge based nanocomposites have been synthesized by various synthesis routes like hydrothermal method, solvothermal method, sonochemical synthesis route, ligand based synthesis etc. Further research and development is in progress for synthesizing better materials through economical methods so that they could find commercial applications.

Lead chalcogenides (especially PbTe) are one of the best candidates for TE devices operating at temperature range up to 600-900 K [8]. Most of the methods used in synthesis of lead chalcogenides are performed at 120-360℃ [9]. Here in this study, a simple route of synthesis of lead chalcogenides at room temperature is reported which provide an economic way to produce PbSe and PbTe materials.

Chapter 2

Literature survey

2.1 Thermoelectric Effects

Thermoelectric effects are phenomena which explain direct energy conversion from heat into electricity and vice versa. The effect was first observed and studied by Thomas J. Seebeck in 1821. After Seebeck, Jean Peltier and William Thomson (Lord Kelvin) contributed in this direction.

2.1.1 Seebeck effect

German physicist Thomas J. Seebeck discovered that if a metal bar is exposed to a temperature gradient (e.g., heating of the one junction and cooling the other), an emf (electro-motive force) is developed between the two ends. Later, it was found that when two dissimilar materials are electrically connected and junctions are held at different temperatures a compass needle kept beside the setup is deflected. It is described as; charge carriers (holes or electrons) at the hot junction at higher thermal velocities diffuse to the cold junction and immobile opposite charges are left at hot side. Due to this separation of charge carriers an emf is produced as shown in Figure 2.1.

Figure 2.1: Charge transportation from the hot to cold end for negative Seebeck co-efficient materials [8].

The whole systems is said to be in quasi-equilibrium state i.e. chemical potential (μ) due to the concentration gradient is countered by the electrostatic potential. This potential is known as Seebeck voltage [10]. The change in electrochemical potential $(\partial\mu)$ in direction of diffusion, per unit temperature ∂T per unit charge 'e' is defined as Seebeck coefficient (S) [11]:

$$\mathbf{S} = \frac{\mathbf{1}}{\boldsymbol{e}} \frac{\boldsymbol{\partial \mu}}{\boldsymbol{\partial T}} \quad (1)$$

The magnitude of the emf produced between the two junctions is directly proportional to the temperature difference ΔT through the linear relationship with the Seebeck coefficient (S) for the material.

$$\mathbf{\Delta V = S\ \Delta T} \quad (2)$$

Seebeck coefficient (S) is an intrinsic property of materials. Metals have very low value of S (only a few μV/K) and semiconductors have comparatively larger values of S (a few hundred μV/K) [12]. Enhanced value of Seebeck coefficient can be achieved by doping in semiconductors. N-type semiconductors have negative Seebeck coefficient because charge carriers are electrons hence direction of heat flow and that of current flow is opposite to each other while in case of P-type semiconductor heat flow and current flow are in same direction hence have a positive S value. A schematic diagram for Seebeck effect is given below (Fig 2.2) in which the junctions of P-type and N-type thermoelectric semiconductors are exposed to temperature gradient and setup is working in power generation mode.

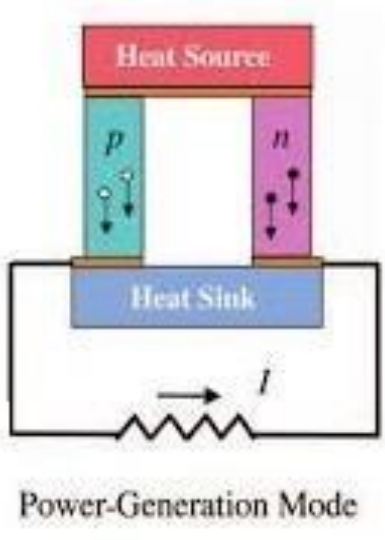

Figure 2.2: Schematic diagrams for thermoelectric module in power generation mode (Seebeck Effect).

2.1.2 Peltier effect

Peltier discovered the reverse of the Seebeck effect in 1834. He observed that by passing a current through two junctions, a temperature difference can be created. He observed that when an electrical current is passed through the junction of two dissimilar materials, heat is

either absorbed or rejected at the junction, depending on the direction of the current. This effect is mainly because of the difference in Fermi energies of the two materials.

A relationship can be established between these two effects which is given by the definition of the Peltier coefficient

$$\Pi = ST \tag{4}$$

At the junction the rate of rejection of Peltier heat (Q_P) is given by

$$Q_P = SIT \tag{5}$$

where I is the current through the junction and T is the temperature in kelvin. So peltier coefficient can be defined as ratio of heat liberated and current through the circuit as

$$\Pi = \frac{Q_P}{I} \tag{6}$$

It is different from Joule heating. In case of Joule heating the current increases the temperature of the material in which it flows but in Peltier effect, a temperature difference is created i.e.one junction becomes cooler and other junction becomes hotter (Fig. 2.3).

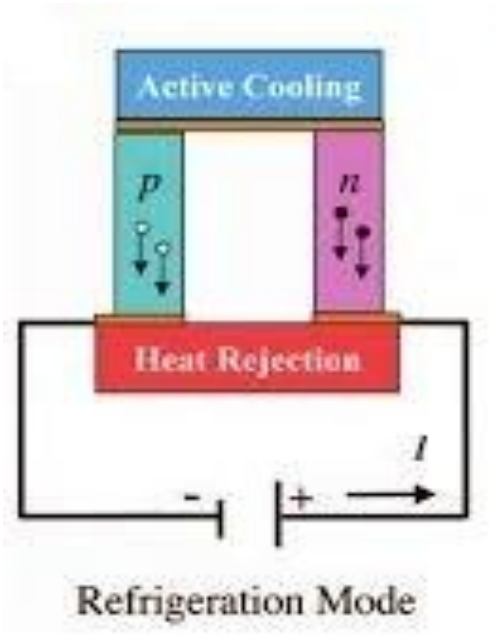

Figure 2.1: Schematic diagram for thermoelectric module in refrigeration mode (Peltier effect).

2.1.3 Thomson effect

Thomson effect is named after William Thomson (Lord Kelvin). It defined as the rate of heat emitted or absorbed in a current carrying conductor subjected to a temperature gradient. Metals such as zinc and copper have a hotter end at a higher potential and a cooler end at a lower potential. When current moves from the hotter end to the cooler end, it is moving from high to a low potential, so there is liberation of heat. This is called the positive Thomson effect. Metals such as cobalt, nickel and iron have a cooler end at a higher potential and a hotter end at a lower potential. When current moves from hotter end to cooler end, it is moving from low to a high potential, and there is absorption of heat. This is called the negative Thomson effect. In lead, there is approximate zero Thomson effect.

If a current density J passes through a homogeneous conductor, heat production per unit volume q is

$$q = \rho J^2 - \mu J \frac{dT}{dx} \tag{8}$$

where,

$\rho \rightarrow$ resistivity of material

$\frac{dT}{dx} \rightarrow$ Temperature gradient along the conductor

$\mu \rightarrow$ Thomson coefficient

The first term in equation given above $\rho.J^2$ (RI^2/V) represents Joule heat per unit volume, which is not reversible.The second term, $\mu.J.\frac{dT}{dx}$, is the Thomson heat, which changes the sign when J changes the direction. The reversible nature of the Thomson effect manifests itself in its mathematical form.

The absolute Seebeck coefficient (S), Peltier coefficient (Π) and Thomson coefficient (μ) are related to one another by Thomson (or kelvin) relationship as given below:

$$S = \frac{\Pi}{T} \tag{9}$$

$$\frac{dS}{dT} = \frac{\mu}{T} \tag{10}$$

2.2 Performance parameters of thermoelectric materials

Thermoelectric (TE) materials convert thermal energy into electrical energy and vice versa, this way they provide an alternative method for power generation and refrigeration. It is required to select a material with higher conversion efficiency i.e. a material which can convert one form of energy into another form effectively. Performance parameter for conversion of heat energy into electrical energy (i.e. in power generation mode) is called thermoelectric efficiency (η) and given as [13]:

$$\eta = \frac{T_H - T_C}{T_H}\left[\frac{\sqrt{(1+ZT_{avg})}-1}{\sqrt{(1+ZT_{avg})}+\frac{T_C}{T_H}}\right] \quad (11)$$

In refrigeration mode conversion efficiency is called coefficient of performance (COP) and given as[13]:

$$\text{COP} = \frac{T_C[\sqrt{1+ZT_{avg}}-\frac{T_H}{T_C}]}{(T_H-T_C)[\sqrt{1+ZT_{avg}}+1]} \quad (12)$$

where,

T_H : temperature at hot side of junction

T_C : temperature at cold side of junction

T_{avg} : average temperature

It is obvious that performance parameters are dependent on a quantity ZT. It is called figure of merit and given as [14].

$$\text{ZT} = \frac{S^2\sigma T}{\kappa} \quad (13)$$

where,

S : Seebeck coefficient (known as thermo power)

σ : Electrical conductivity

κ : Thermal conductivity

Z : Power factor ($Z = S^2\sigma/\kappa$)

From equation (1) and (2), it is clear that Seebeck coefficient is not the only quantity that determines the potential of a material for its application as thermoelectric materials but it is Figure of merit (ZT) which plays a significant role in deciding the usefulness of material in thermoelectric (TE) applications.

A good thermoelectric material must have high value of figure of merit. Theoretically there is no maximum value for figure of merit (ZT). We can observe from equation (1) that ZT can vary from zero to infinity.

When,

ZT = 0 $\rightarrow \eta = 0$

ZT = infinite $\rightarrow \eta = \frac{T_H - T_C}{T_H}$ (14)

Equation (14) is called Carnot efficiency and it is maximum efficiency that is theoretically possible. It is also observed from equation (1) that conversion efficiency increases with increment in ZT as shown in Fig 2.4. It shows the variation of thermoelectric energy conversion efficiency of a thermoelectric device (heat engine) as a function of figure of merit (ZT) when temperature of cold junction is kept at room temperature.

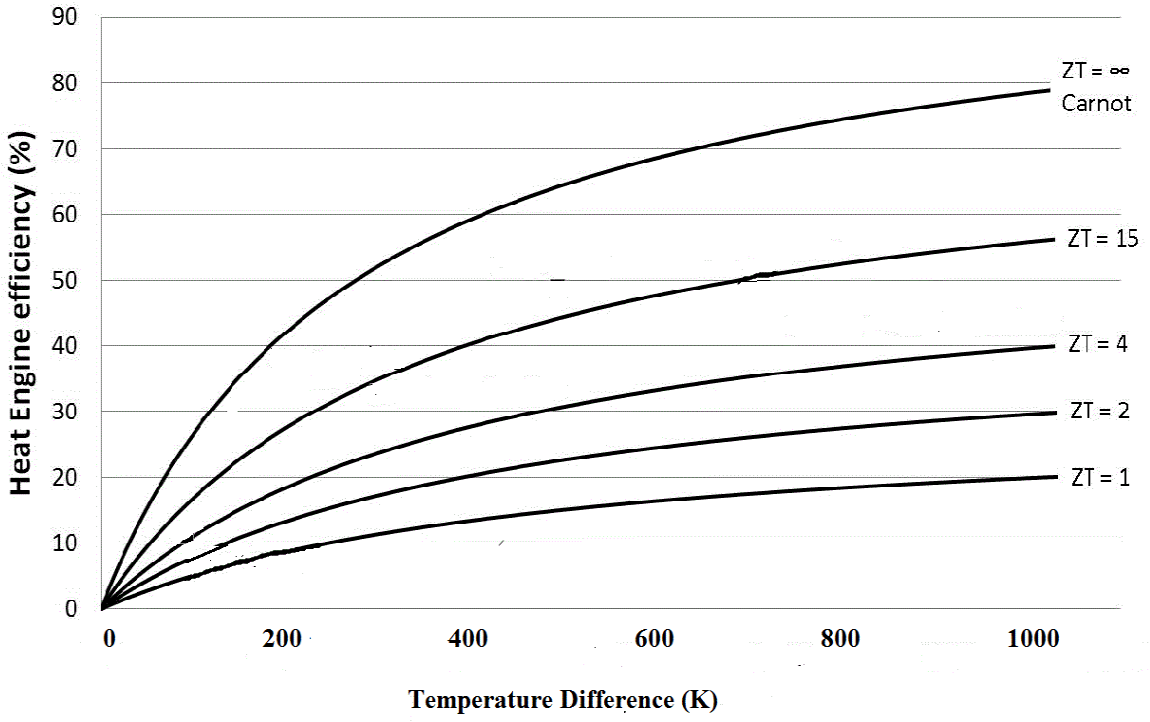

Figure 2.4: Thermoelectric energy conversion as a function of ZT at the setting of cold junction temperature T_C = 300 K [15].

For efficiency improvement, there is a need of high ZT value and simultaneously high temperature difference between hot junction and cold junction. While keeping temperature difference higher than 1200 K is very difficult for practical reasons but there are no such limitations for ZT value.

Regardless of such a high expectation and accomplishments, the advancement in thermoelectric materials has still been restricted for commercial applications because thermoelectric materials synthesized so far possess low value of ZT. Commercially available thermoelectric materials have ZT ≈ 1, so they provide a conversion efficiency of 5-10 % depending on temperature difference between junctions. As can be seen, there is an incredible potential to look for new materials with ZT estimations of 2–3 to give the fancied transformation efficiencies. For example, a thermoelectric power conversion device with ZT = 3 operating between 500˚C (773 K) and 30˚C (303 K) would give a Carnot efficiency of 50 % approximately [16]. Consequently, it is important to synthesize thermoelectric materials with high ZT keeping in mind the end goal to advance the viable uses of thermoelectric materials.

2.3 Challenges in enhancing figure of merit (ZT)

Performance parameter of any thermoelectric material i.e. figure of merit (ZT) depends on many quantities such as:

$$\mathbf{ZT} = \frac{\boldsymbol{S^2\sigma T}}{\boldsymbol{\kappa}} = \frac{\boldsymbol{S^2 T}}{\boldsymbol{\kappa\rho}} \tag{15}$$

Hence, different quantities like Seebeck coefficient (S), electrical conductivity (σ), thermal conductivity (κ) and temperature difference between junctions (T) that can be varied in order to achieve optimum value of ZT. Enhancement of ZT has been a crucial task for researchers for more than 60 years, because of interdependency of various parameters. Various issues are discussed here.

Seebeck coefficient S is defined as the energy difference between the average energy of mobile carrier and the Fermi energy [17]. If the carrier concentration (n) is increased, the Fermi energy as well as the average energy increases but this increment is more rapid in case of Fermi energy in comparison to increment in average energy. Therefore S decreases with increase in carrier concentration and power factor ($S^2\sigma$) decreases more rapidly. Therefore, for most of the homogeneous materials, increase in carrier concentration (n) increases electrical conductivity (σ) but simultaneously reduces the Seebeck coefficient (S). For this reason, in metals and degenerate semiconductors (energy-independent scattering approximation), the Seebeck coefficient can be expressed as [18].

$$S = \frac{8\pi^2 k_B^2}{3eh^2} m^* T \left(\frac{\pi}{3n} \right)^{2/3} \quad (16)$$

Where,

k_B→ Boltzmann constant

e → carrier charge

h → planck constant

m^*→effective mass of charge carrier

n → carrier concentration

The Seebeck coefficient as well as ZT is directly proportional to effective mass m^* according to the Eq. (16). So it seems that materials having high m^* should have higher ZT values but in practical scenario most of the materials having high effective mass (m^*) possess low carrier mobility (μ) which curbs the power factor and hence ZT, by a weighted mobility as defined by relationship given as [13]:

$$S^2\sigma \propto (m^*)^{3/2}\mu \quad (17)$$

Also, drawback with effective mass is that it can not be optimized. There are materials with low mobility and high effective mass polaron conductors (oxides, chalcogenides) as well as materials with high mobility and low effective mass semiconductors like SiGe, GaAs [19].

Thermal conductivity (κ) in equation (15) is represented as $\kappa = \kappa_e + \kappa_l$ where κ_e is electronic thermal conductivity and κ_l is lattice thermal conductivity. From the Eq. (15), it is observed that if $\kappa \to 0$ then ZT → ∞ and the thermoelectric devices tend to achieve maximum efficiency i.e. the Carnot cycle efficiency. In ZT, electrical conductivity (σ) and electronic thermal conductivity (κ_e) comes due to motion of energy carriers like electrons and holes while lattice thermal conductivity (κ_l) comes because of diffusion of phonons (quanta of heat). According to Wiedemann–Frenz Law [19] the electronic thermal conductivity is directly proportional to the electrical conductivity of the materials and the relationship is given as

$$\kappa_e = L\,\sigma\,T \quad \leftrightarrow \quad (\kappa_e/\sigma) = LT \quad (18)$$

Where L is Lorenz No. which is a constant and value for free electrons is given as 2.4×10^{-8} J^2/K^2C^2 so at the same temperature LT has a fixed value hence (κ_e /σ) has same value for

different metals. When carrier concentration is increased, electrical conductivity σ also increases according to expression:

$$\sigma = ne\mu \tag{19}$$

but simultaneously κ_e also increases and no improvement in ZT is observed. Again from equation (16), it is shown that increasing the effective mass of the carrier increases S but reduces the carrier mobility and hence the electrical conductivity σ according to equation (19).

Consequently, it is obvious that any attempt to increase σ, will also result an increase in κ_e which contributes to thermal conductivity (κ) and no significant improvement in ZT can be achieved. Therefore in attempt to decrease thermal conductivity κ, more focus is on decreasing κ_l which can be decreased by various approaches.

The expression for κ_l is given as [13]

$$\kappa_l = \frac{1}{3}(C_v\, v_s\, \lambda_{ph}) \tag{20}$$

where,

C_v : heat capacity

v_s : sound velocity

λ_{ph}: phonon mean free path

So, this parameter is independent of electronic structure of material and can be altered in order to maximize ZT. But, decreasing κ_l with enhanced phonon scattering by introducing structural defects results in decrease in carrier mobility hence in electrical conductivity because defects scatter the phonons as well as the electrons. Subsequently there are some trade-offs followed up in carrier mobility when designing for decreasing lattice thermal conductivity. Therefore not only κ_l but also ratio of μ/κ decides the improvement of ZT [20]. Although the improvement in the ratio μ/κ is generally achieved through a reduction in κ_l rather than that in μ. some basic issues related to this mechanism are not defined well.

These are the major issues reported by researchers in attempt to improving the bulk materials properties for using them as commercial purpose TE material. The main focus has been spent on reducing the lattice thermal conductivity by manipulation of

phonon scattering mechanism in bulk materials and low dimensional materials [21]. Spitzer reports that for semiconductors, the lower limit for the κ_l is 0.2 W/mK [22]. Due to such restriction over κ_l, there are suggestions to utilize the electronic thermal conductivity rather than lattice thermal conductivity. The distribution of charge carriers (of a given energy during transport process) with zero variance i.e. close to mean value is called Dirac delta distribution. At this narrow band, κ_e can be minimized without any significant decrease in the electric conductivity σ. These narrow bands produce high effective masses that results the larger Seebeck coefficient and hence the enhanced ZT [22].

Apart from the reducing the thermal conductivity, minimum values of some other parameters such as S ~150 mV/K should also be achieved in order to achieve the ZT~ 1. If does not so, it is irrelevant that material possess the lowest thermal lattice conductivity [23]. On concluding from explanations given above, that ideal thermo-electric materials should have a very narrow distribution of energy carriers, the defects to scatter phonons and high carrier velocity in the direction of the applied field, in order to enhance ZT. However, it was postulated by Pichanusakorn et al. that sheer magnitude is deciding factor not the shape of DOS [17].

It is also observed that commercially available TE materials having ZT~1 can not perform good at a relatively larger temperature lift or difference ($T_H - T_C$), e.g. 30˚C but, when temperature lift is decreased, the efficiency of thermoelectric systems increases rapidly. It is expected when temperature lift is very small such as 5˚C, the thermoelectric modules could give a strong competition to traditional vapor compression systems [24]. Moreover, it is encouraging to know that the second law of thermodynamics does force any limitation on enhancing the value of ZT and yet, it has been a challenging task for researchers to synthesize materials having ZT beyond certain point [25].

2.4 Basic theory and methodology for improving figure of merit

From equation (15), it is clear that for high ZT values material should have a large Seebeck coefficient, and a high electrical conductivity. Metals (conductors) possess very low S value in the order of 1-10 μV/K (less than characteristic value i.e. 87 μV/K) [8] but high electrical conductivity, while in case of insulators and semiconductors large S value and low conductivity is found. A plot is drawn in fig 2.5 showing various parameters [26].

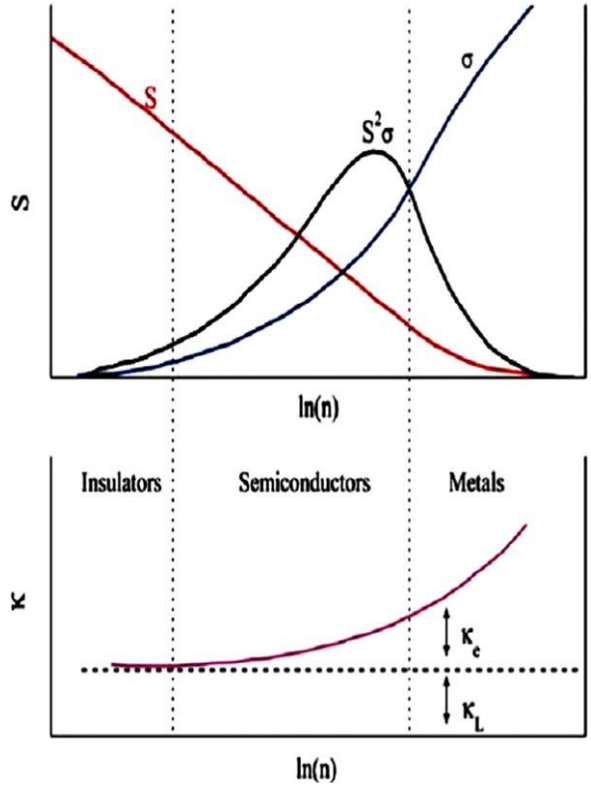

Figure 2.5: The variation of the Seebeck coefficient (S), electrical conductivity (σ), power factor ($S^2\sigma$), electronic thermal conductivity (κ_e) and lattice (κ_l) thermal conductivity on the charge carrier concentration n, for a bulk material [26].

It can be concluded from graph that maximum thermoelectric power factor can be achieved somewhere between the carrier concentrations of metals and that of semiconductors. Generally heavily doped semiconductors (carrier concentration of 10^{19}–10^{21} cm^{-3}) serve as good thermoelectric materials [27]. To ensure large Seebeck coefficient, dopant atoms should be of same type either n-type or p-type because mixed n-type and p-type charge carriers produces an opposing Seebeck effect and hence ZT is reduced. Therefore to ensure single type of carriers, selected semiconductors materials should be with appropriate energy bandgaps and suitable doping, so that their doped version i.e. n-type and p-type can be well distinguished. In order to achieve high carrier mobility and single carrier type heavily doped semiconductor materials with energy bandgap energy (E_g) less than 1 eV are used as efficient TE materials. Seebeck coefficient, electrical conductivity and Decoupling of the thermal conductivity and electronic conductivity, has been key factors to improve ZT.

For more efficient materials we need to focus on reducing the thermal conductivity by introducing scattering points (eg. voids, rattlers etc.) and increasing power factors ($S^2\sigma$). These parameters are the function of scattering factor r, carrier effective mass m^*

and carrier mobility (μ) and their interconnectivity limit ZT to about 1 in large bulk materials. Two primary methodologies are being implemented mainly in searching for efficient thermoelectric materials. The first approach is named as the ‘‘phonon glass electron crystal’’ (PGEC) approach and the other approach is the nanostructuring of TE materials.

2.4.1 PGEC thermoelectric materials

PGEC approach suggests that an ideal TE material should possess the thermal conductivity as in glass and electronic properties as in crystal [28]. In typical PGEC materials, electrons are able to carry charge and heat freely due their high mobility and uninterrupted movement, while the phonons are interrupted from carrying heat at the atomic scale. This approach can be easily achieved in complex crystal structures with vacancies (voids) and large amount of interstitial sites filled with other heavy element atoms known as ‘‘rattler’’. Voids help in scattering phonons while rattlers vibrate at low frequencies by consuming thermal energy. This way, these vacancies and rattlers disrupt heat energy advancement within the material and reduce the lattice thermal conductivity. Therefore, the PGEC materials act like a crystal for electrons ensuring smooth movement but scatter phonons effectively as in glass material. This property enables these materials offering high electrical conductivities but low thermal conductivities. Typical examples of PGEC thermoelectric materials are skutterudites [29,30], clathrates [31,32] **etc**.

2.4.2 Nanostructured TE materials

The second approach suggests that the ZT can be improved with nanostructured morphologies [33-35]. Quantum confinement effect occurred in nanostructures can enhance the density of states (DOS) near Fermi level hence increase the thermopower. Therefore it provides a method to decouple thermal conductivity and electrical conductivity [33-35]. Nanostructuring also increases phonon scattering by introducing a large density of interfaces. Since mean free path (mfp) of phonons is much longer than that of electrons in heavily doped semiconductors, so phonons can be scattered more effectively over a large mean free path (mfp) range, as illustrated in Fig. 2.6.

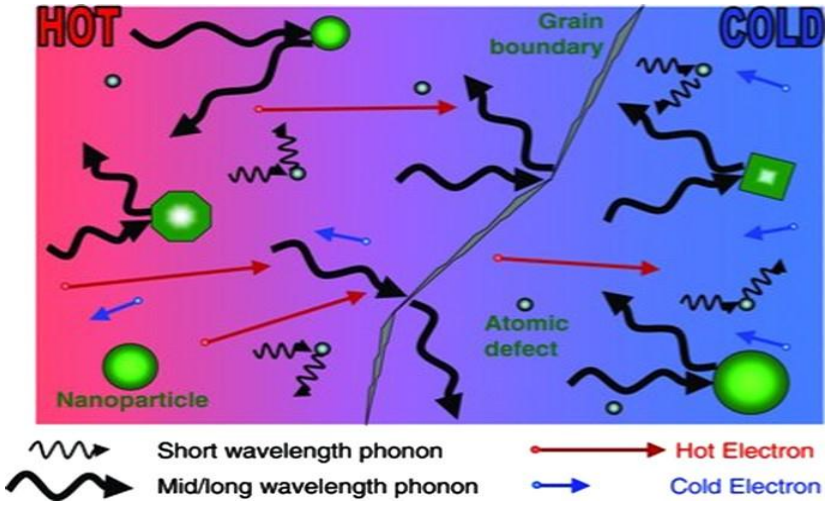

Figure 2.6: Schematic diagram illustrating phonon scattering mechanisms and electronic transport of hot and cold electrons within a thermoelectric material [36].

This way lattice thermal conductivity is reduced effectively while carrier mobility and electronic conductivity remains unaltered [34]. This type of nanostructuring can be achieved by making one or more dimensions smaller than the mean free path of phonons, while still larger than that of charge carriers. Significant ZT enhancement has been found in two-dimensional (2D), one- dimensional (1D) and nanocomposite thermoelectric materials.

With low dimensional materials it is advantageous with anisotropic Fermi surfaces in multi valley cubic semiconductor and increased mobilities at a given carrier concentration when the quantum confinements are satisfied so that modulation doping and delta doping can be utilized. Thus they give us freehand to manipulate the thermoelectric parameters. The another aspect is that the low dimensional particles are promising candidates in increasing ZT also because Wiedmann-Franz law is not applicable to nanomaterials with delta like DOS [37]. The carrier mobility μ is independent of electron–phonon coupling under the normal condition such as near and above the room temperature [38]. Hence phonon drag has been ignored in the most of the calculation in these temperature regions [39].

Hence, nanotechnology gives a hope for economic, ecofriendly and commercial purpose large scale thermoelectric power generations along with solving other heat related issues.

2.5 Lead chalcogenides as thermoelectric materials

Lead chalcogenides (PbX, X = group VI elements especially Se and Te) have shown a promising usefulness as thermoelectric materials. PbX are direct bandgap semiconductor materials, possess very small band gap (E_g = 0.28 eV for PbSe and 0.31 eV for PbTe at RT) and a large Bohr excitation radius (46 nm for PbSe and PbTe) [9], which show broad quantum size effects at nanoscale and have been extensively used in various fields including as thermoelectric materials [40-43].

Structure of lead chalcogenides is cubic like NaCl. Each Pb atom is surrounded by six Se/Te atoms and each Se/Te atom is surrounded by six Pb atoms. The isotropic structure of lead chalcogenides provides uniform thermoelectric properties in all directions.

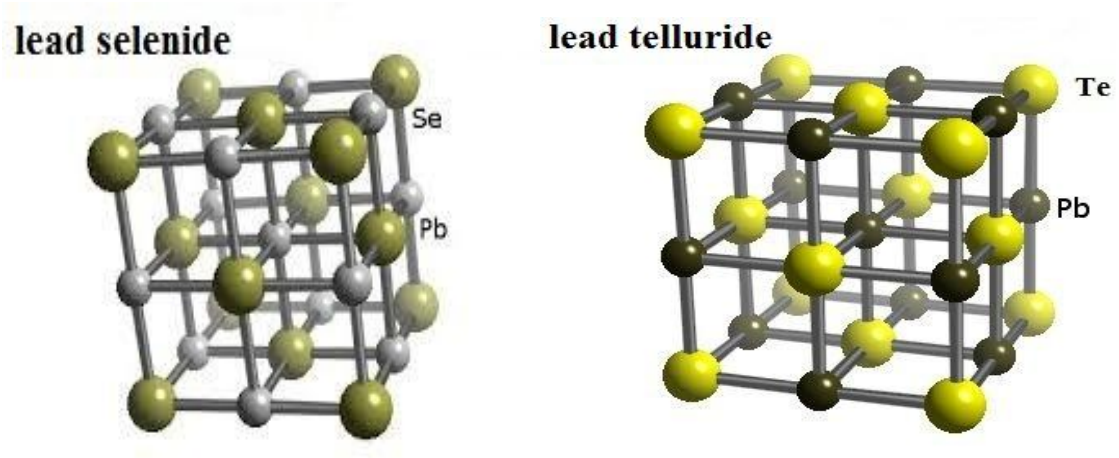

Figure 2.7: crystal structure of lead chalcogenides.

Lead chalcogenides have high melting points for example melting point of PbTe is 923℃ as compared to 585℃ for Bi_2Te_3, hence have great potential for TE application over a wide range of temperature of 100-1400 K. For lead telluride, maximum ZT = 0.8 is reported at 800 K approximately so it can be used for power generation in the temperature range of 600-900K.

It is reported that nanoscaled lead materials show improved performance in comparison with their bulk counterparts.This approach of improving ZT was introduced by Kicks and Dresselhaus when they achieved improved ZT in 2-D Bi_2Te_3 quantum well due to occurance of quantum confinement effect in in the interlayer direction hence increased DOS near the Fermi level and enhanced thermopower [44]. Further they suggested that if layer thickness of Bi_2Te_3 was less than mean free path of phonon then phonons would be

effectively scattered by interfaces between layers and thermal conductivity would be decreased [44,45].This nanostructuring approach is considered as a promising method and implemented for various TE materials including lead chalcogenides and have shown adequate improvement in thermopower. Various nanoscaled structures of lead chalcogenides like nanorods [46,47], nanocubes [48,49], nanoparticles, nanotubes [50,51], nanoflowers [52], have been synthesized successfully and morphology can be controlled through varying experimental conditions. These nanostructures shows improved ZT in comparison to their bulk counterparts (maxium ZT = 0.34 for PbSe, 0.8 for PbTe), for example Harman and coworkers demonstrated ZT = 1.6 in PbTe-PbSeTe system which they described as PbSe nanodots dispersed in a PbTe matrix [53].

Lead chalcogenides based nanocomposites have also shown a significantly great increase in ZT value as ZT ~ 2.2 was reported by K. F. Hsu and coworkers in PbTe based composite $Ag_{1-x}Pb_{18}SbTe_{20}$ (LAST) [54]. LAST alloys contain Ag-Sb nanostructures which help in lowering thermal conductivity. A number of other nanocomposites are also reported having ZT value greater than one for example $AgPb_mSn_nSbTe_{2+m+n}$(LASTT), $NaPb_mSbTe_{2+m}$(SALT-m), KPb_mSbTe_{m+2}(PLAT-m) etc [55-57].

Chapter 3

Experimental

3.1 Synthesis of Lead chalcogenides (PbSe, PbTe)

various methods are being implemented for synthesizing thermoelectric material in order to seeking an economically efficient method. Hydrothermal and solvothermal technique is performed under high temperature and high pressure condition in a sealed flask. Sonochemical process gives highly crystalline chalcogenides such as PbS, PbSe, Bi_2Se_3 but tellurides are difficult to be synthesized by this method. Ligand based method required organic ligands like TOPO (trioctylphosphine oxide). All these methods are promising methods for achieving morphologically controlled nanostructures but a synthesis route which is performed under ambient conditions and in inorganic solutions might be a good alternative for low cost synthesis for commercial purpose synthesis. Here a cost effective, room temperature synthesis of lead chalcogenides has been reported and synthesis is performed in inorganic solutions.

The synthesis of lead chalcogenides has been carried out in following steps:

1) 20 ml hydrazine hydrate (NH_2NH_2 .H_2O) and appropriate amount of NaOH pellets were taken in a 100 ml glass beaker.
2) This mixture was kept on a magnetic stirrer at room temperature, at 500 rpm for 90 minutes to get a hydrazine hydrate saturated alkaline solution.
3) 2 mmol chalcogen (Se, Te) was added immediately and solution was kept under continuous stirring for next 30 minutes.
4) 2 mmol lead nitrate {Pb($NO_3)_2$} was added and stirring was continued for next 15 minutes, then solution became black.
5) This solution was kept at room temperature under ambient pressure condition for next 36 hours.
6) Black precipitate was filtered and washed by HNO_3 (pH=3) and then deionized water for several times.

A flow chart given below summarizes the experimental procedure for synthesis.

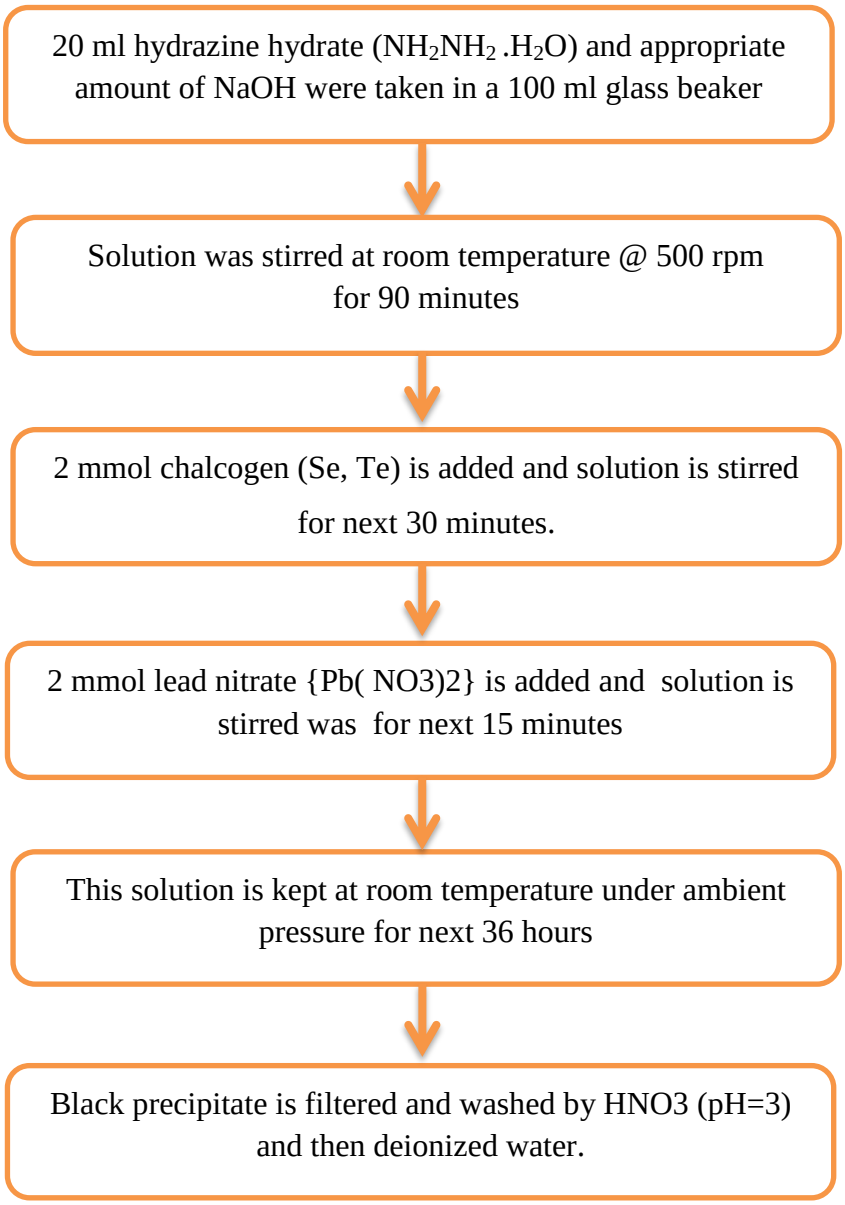

3.2 Characterisation Techniques

After synthesis, for phase confirmation and morphological measurement were carried out using X-Ray diffraction method and scanning electron microscopy techniques.

3.2.1 X-Ray diffractometer

Up to 1895 the study of matter at the atomic level was a difficult task but the discovery of electromagnetic radiation with 1 Å (10^{-10} m) wavelength, appearing in the region between gamma-rays and ultraviolet, makes it possible. As the atomic distance in matter is

comparable with the wavelength of X-ray, the phenomenon of diffraction find its way through it and gives many promising results related to the crystalline structure.

Crystals are regular arrays of atoms, and X-rays can be considered waves of electromagnetic radiation. Atoms scatter X-ray waves, primarily through the electrons. X-ray striking an electron produces secondary spherical waves emanating from the electron. This phenomenon is known as elastic scattering, and the electron is known as the scatterer. A regular array of scatterers produces a regular array of spherical waves. Although these waves cancel one another out in most directions through destructive interference, they add constructively in a few specific directions, determined by Bragg's law (fig 3.1).

$$2d \sin\theta = n\lambda$$

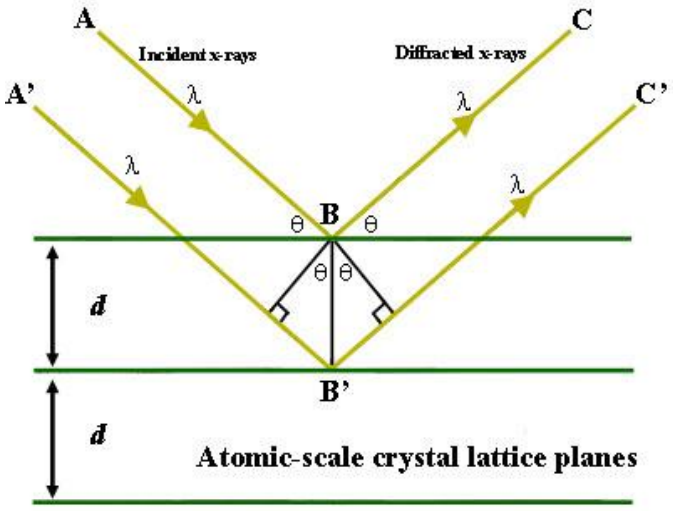

Figure 3.1: X-Ray diffraction in accordance with Bragg's law. [58]

Where *n* is an integer 1, 2, 3….. (Usually equal 1), λ is wavelength in angstroms (1.54 Å for copper), d is interatomic spacing in A°, and θ is the diffraction angle in degrees.

The characteristic of the sample can be determined by plotting the angular positions and intensities of the resultant diffracted peaks of radiation. XRD is used to determine the structure of sample, i.e. how the atoms pack together in the crystalline state and what the interatomic distances and angles are.

The main components of XRD are an X-ray tube, a sample holder, and an X-ray detector. X-rays are generated in a cathode ray tube by heating a filament to produce electrons, accelerating the electrons toward a target by applying a voltage, and bombarding the target material with electrons. When electrons have sufficient energy to dislodge inner

shell electrons of the target material, characteristic X-ray spectra are produced. These spectra consist of several components, the most common being K_α and K_β. K_α consists, in part, of $K_{\alpha 1}$ and $K_{\alpha 2}$. $K_{\alpha 1}$ has a slightly shorter wavelength and twice the intensity as $K_{\alpha 2}$. The specific wavelengths are characteristic of the target material (Cu, Fe, Mo, Cr). Filtering, by foils or crystal monochrometers, is required to produce monochromatic X-rays needed for diffraction. $K_{\alpha 1}$and $K_{\alpha 2}$ is sufficiently close in wavelength such that a weighted average of the two is used. Copper is the most common target material for single-crystal diffraction, with Cu K_α radiation = 1.5418Å [59]. These X-rays are collimated and directed onto the sample. As the sample and detector are rotated, the intensity of the reflected X-rays is recorded. When the geometry of the incident X-rays impinging the sample satisfies the Bragg Equation, constructive interference occurs and a peak in intensity occurs. A detector records and processes this X-ray signal and converts the signal to a count rate which is then output to a device such as a printer or computer monitor. The geometry of an X-ray diffractometer is such that the sample rotates in the path of the collimated X-ray beam at an angle θ while the X-ray detector is mounted on an arm to collect the diffracted X-rays and rotates at an angle of 2θ. The instrument used to maintain the angle and rotate the sample is termed a goniometer.

Figure 3.1: X-Ray diffractometer Brucker D8 advance

X-Ray diffractometer of Brucker model: D8 advance was used to obtain X- ray patterns (Figure 3.2). For typical powder diffraction patterns, in this study data is collected between diffraction angle 2θ vs intensity of X-ray in a wide range of angle 10° to 70° using $CuK_{\alpha 1}$ radiation of wavelength, 1.54 Å at the scan rate of 2 deg/min.

3.2.2 Scanning electron microscopy

A scanning electron microscope (SEM) is a type of electron microscope that produces images of a sample by scanning it with a focused beam of electrons as shown in Figure 3.3. The electrons interact with atoms in the sample, producing various signals that can be detected and that contain information about the sample's surface topography and composition. The signals that derive from electron reveal information about the sample including external morphology (texture), chemical composition, and crystalline structure and orientation of materials making up the sample. In most applications, data are collected over a selected area of the surface of the sample, and a two-dimensional image is generated that displays spatial variations in these properties. The electron beam is generally scanned in a raster scan pattern, and the beam's position is combined with the detected signal to produce an image.

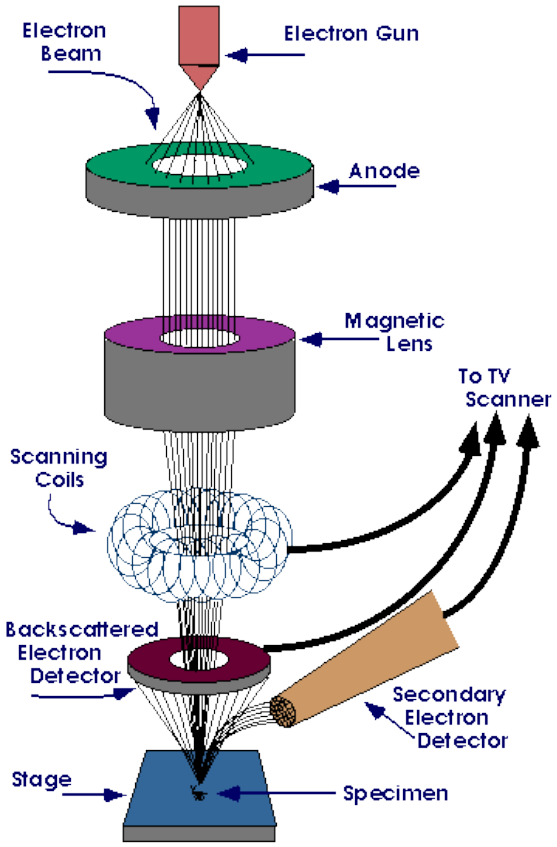

Figure 3.3: Schematic diagram of SEM assembly. [61]

A typical SEM consists of electron gun, electron lenses, sample stage, detector for all signals of interest, display/data output devices as shown in In most applications, data are collected over a selected area of the surface of the sample, and a 2-dimensional image is generated that displays spatial variations in these properties. Areas ranging from approximately 1 cm to 5 microns in width can be imaged in a scanning mode using

conventional SEM techniques (magnification ranging from 20X to approximately 30,000X, spatial resolution of 50 to 100 nm) [60]. The SEM is also capable of performing analyses of selected point locations on the sample; this approach is especially useful in qualitatively or semi-quantitatively determining chemical compositions (using EDS), crystalline structure, and crystal orientations (using EBSD). The design and function of the SEM is very similar to the EPMA and considerable overlap in capabilities exists between the two instruments.

The SEM produces a largely magnified image by using electrons instead of light because wavelength of wave associated with electron much shorter than light. A beam of electrons is produced at the top of the microscope by an electron gun. The electron beam follows a vertical path through the microscope, which is held within a vacuum. The beam travels through electromagnetic fields and lenses, which focus the beam down toward the sample. Once the beam hits the sample, electrons and X-rays are ejected from the sample. Detectors collect these X-rays, backscattered electrons, and secondary electrons and convert them into a signal that is sent to a screen similar to a television screen. This produces the final image.

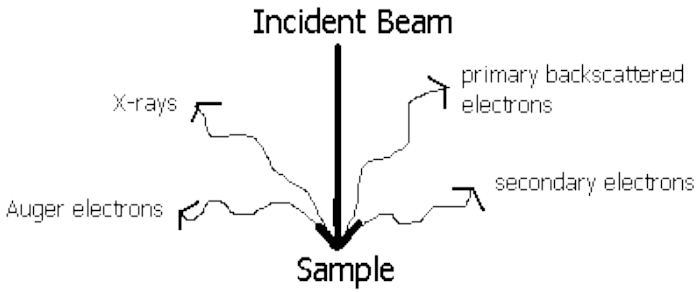

SEM utilizes vacuum conditions and uses electrons to form an image, special preparations must be done to the sample. All water must be removed from the samples because the water would vaporize in the vacuum. All metals are conductive and require no preparation before being used. All non-metals need to be made conductive by covering the sample with a thin layer of conductive material. This is done by using a device called a "sputter coater."

The sputter coater uses an electric field and argon gas. The sample is placed in a small chamber of it is at a vacuum. Argon gas and an electric field cause an electron to be removed from the argon, making the atoms positively charged. The argon ions then become attracted

to a negatively charged gold foil. The argon ions knock gold atoms from the surface of the gold foil. These gold atoms fall and settle onto the surface of the sample producing a thin gold coating.

Figure 3.4: Hitachi S-3700 N scanning electron microscope.

Hitachi made S-3700N SEM system shown in figure 3.4 is used in the study of lead based TE materials. Operating voltage was kept at 15 kV. Since lead chalcogenides are semiconductor, gold coating was done to make sample conducting.

Chapter 4

Results and discussion

Characterization of the synthesized PbSe and PbTe nanocubes is carried out by XRD, SEM and EDS. XRD patterns in Fig 4.1 demonstrate the proper phase formation of PbSe crystal structure and high crystallization of the materials. All diffraction peaks of PbSe sample are indexed to Fm3m space group of face centered cubic structure of pure PbSe and it matches well to literature data (ICDD reference code 01-078-1902). Similarly diffraction peaks of PbTe sample correspond to literature data (ICDD reference code 01-078-1905).

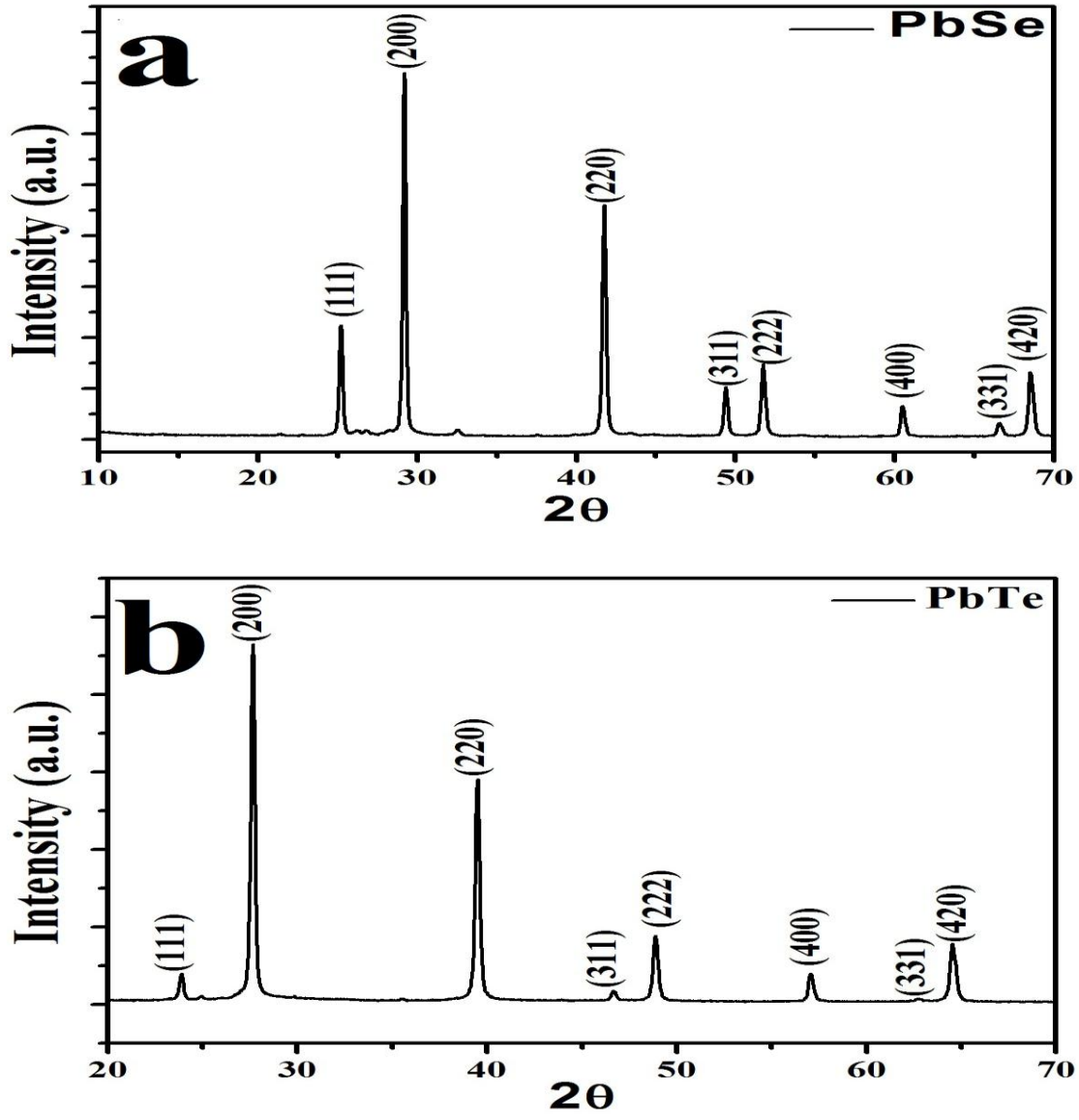

Figure 4.1: XRD spectra of synthesized lead chalcogenides; (a) PbSe (b) PbTe .

Lattice constants estimated from the XRD patterns of PbSe and PbTe are equal to 6.1064 Å and 6.435 Å for PbSe and PbTe respectively. The value of lattice constant a,b and c will be equal in PbSe due to cubic crystal structure. Similarly it is followed by PbTe crystal system. And these values of lattice constant are almost justified by literature data of lattice parameters.

SEM images given below give morphology of synthesized lead chalcogenides nanocubes. Fig 4.2 (a) and (b) exhibit uniformly distributed and slightly agglomerated nanocubes of PbSe in size range of 80-130 nm. Fig 4.2 (c) and (d) exhibit nanocubes of PbTe in size range of 60-110 nm, respectively. Particle size is much smaller in case of PbTe in comparison to that of PbSe.

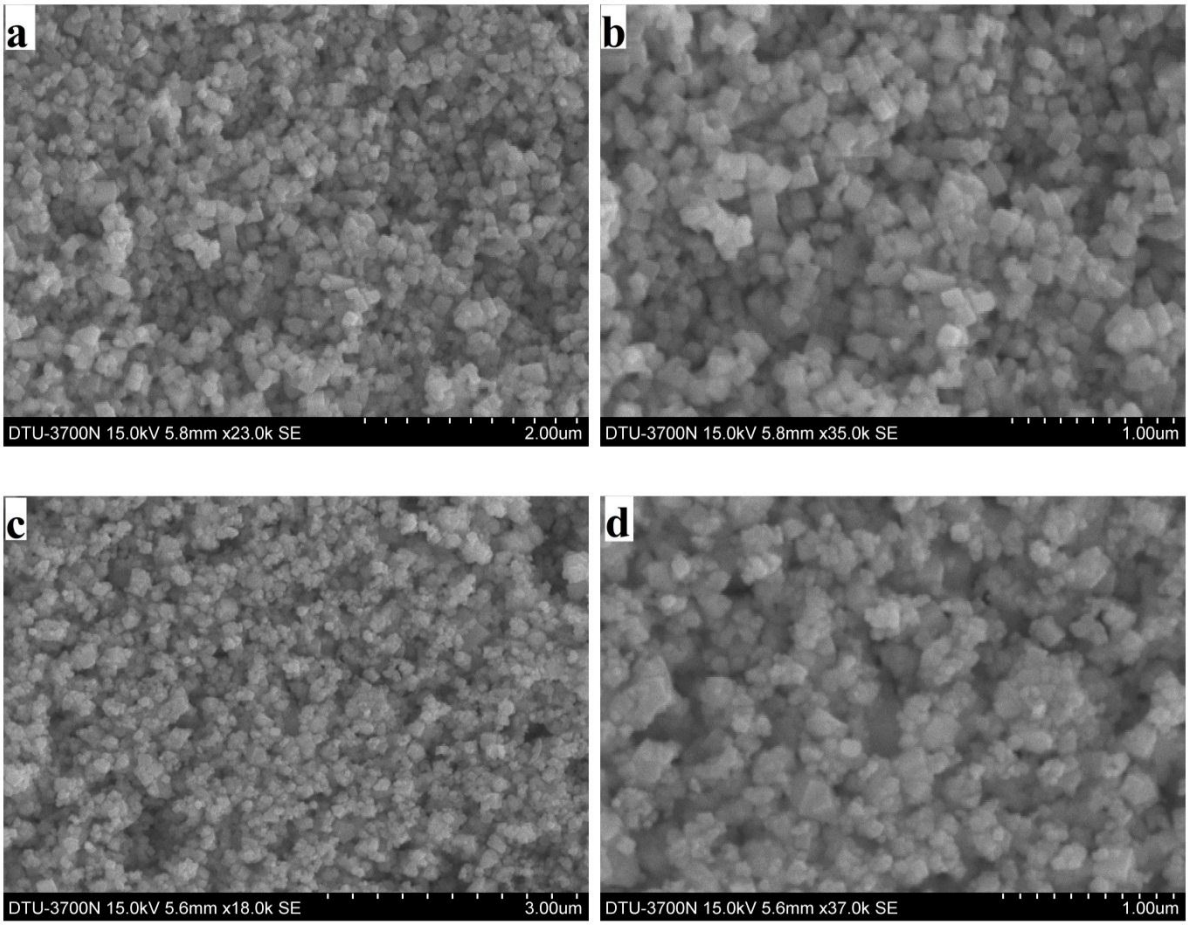

Figure 4.2: SEM micrographs of PbSe in scale (a) 2 μm (b) 1 μm and of PbTe in scale (c) 3μm (d) 1 μm.

EDS measurement of synthesized PbSe and PbTe samples was also performed at 15 KV at take off angle of 66.5 degree to measured the weight percentage and atomic percent of elements in these

chalcogenides are shown in Fig 4.3 and 4.4. Quantitative analysis of EDS as given in Table 4.1 and 4.2 represents the chemical composition of Pb and Se in PbSe is by and large same, similarly Pb and Te in PbTe compositions. It is also confirmed by EDS spectrum that there is no other impurity element present.

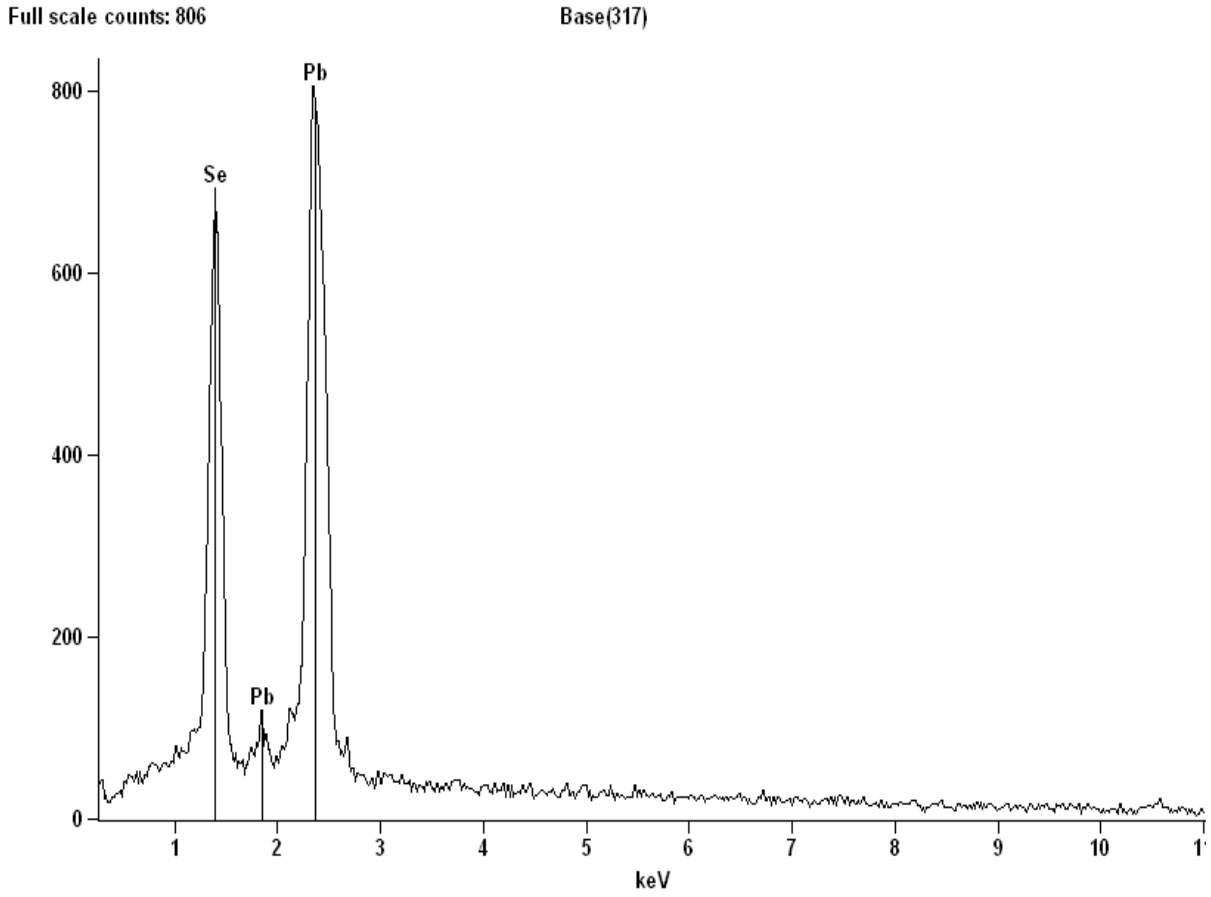

Figure 4.3: EDS spectrum of synthesized PbSe nanocubes.

Table 4.1: Quantitative data of PbSe nanocubes

Element Line	Net Counts	Int. Cps/nA	Weight %	Weight % Error	Atom %	Atom % Error	Formula	Standard Name
Se K	201	---	---	---	---	---		
Se L	8526	---	28.36	+/- 0.57	50.96	+/- 1.03	Se	
Pb L	239	---	---	---	---	---		
Pb M	16739	---	71.64	+/- 1.44	49.04	+/- 0.98	Pb	
Total			100.00		100.00			

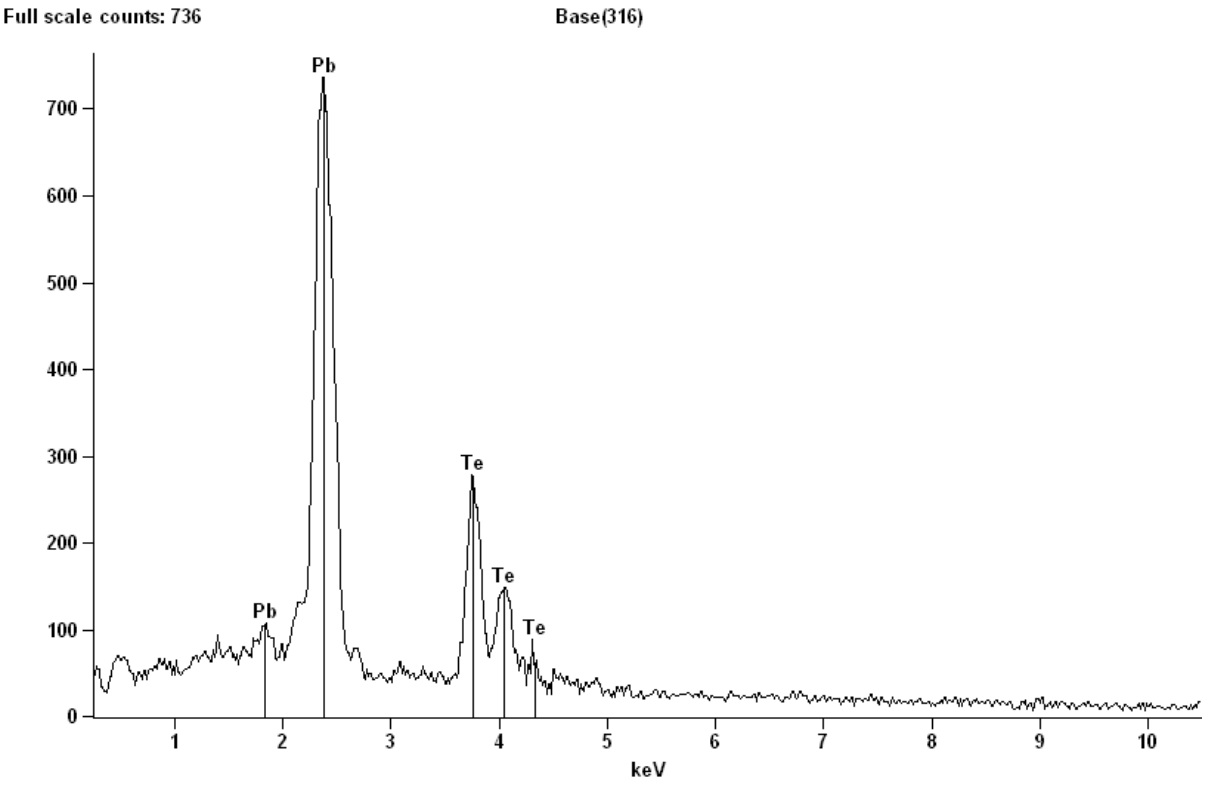

Figure 4.4: EDS spectrum of PbTe nanocubes.

Table 4.1: Quantitative Results of PbTe nanocubes

Element Line	Net Counts	Int. Cps/nA	Weight %	Weight % Error	Atom %	Atom % Error	Formula	Standard Name
Te L	6460	---	43.46	+/- 1.83	55.52	+/- 2.34	Te	
Te M	0	---	---	---	---	---		
Pb L	130	---	---	---	---	---		
Pb M	15045	---	56.54	+/- 1.23	44.48	+/- 0.97	Pb	
Total			100.00		100.00			

A possible chain of reactions can be proposed on the basis of experimental results [9]. According to the electrode potential analysis, in alkaline solutions:

$S + 2e^{--} \rightarrow S^{2--}$ $\quad E^0 = -0.407\ V$

$Se + 2e^{--} \rightarrow Se^{2--}$ $\quad E^0 = -0.924\ V$

$Te + 2e^{--} \rightarrow Te^{2--}$ $\quad E^0 = -1.143\ V$

$N_2 + 4H_2O + 4e^{--} \rightarrow N_2H_4 + 4OH^{--}$ $\quad E^0 = -1.15V$

Hydrazine is a reducing agent and can reduce selenium to bivalent anions, but it can not reduce tellurium effectively because redox potential of tellurium is close to that of hydrazine.

When we make hydrazine solution alkaline by adding NaOH, polytelluride anions of the form $TE_{\alpha+1}^{2-}$ are formed. For other chalcogens also polychalcogenides anions can exist. These polychalcogenides function as chalcogen source and release chalcogen anions which react with Pb^{2+} to form lead chalcogenides. So, the main possible reactions in the synthesis process may include:

$(\alpha+1)X + N_2H_4 + OH^{-} \rightarrow N_2 + 4H_2O + X_{\alpha+1}^{2-}$ (X = Se, Te)

$X_{\alpha+1}^{2-} \rightarrow \alpha X + X^{2-}$

$Pb^{2+} + X^{2-} \rightarrow PbX$

Chapter 5

Summary and Conclusion

In conclusion, a simple solution chemical route at room temperature is demonstrated to the synthesis of lead chalcogenides nanocubes. Characterization of synthesized samples is done by XRD, SEM and EDS. Phase formation is confirmed by XRD spectrum and calculated particle size comes out to be 28.49 nm for PbSe and 30.975 nm for PbTe at highest intensity peak. Surface morphology is investigated by SEM which showed nanocubes of PbSe in size range of 80-130 nm and nanocubes of PbTe in size range of 60-110 nm. Chemical composition is confirmed by EDS which confirmed the absence of any other impurity atom. Lead chalcogenides (PbSe and PbTe) are efficient TE materials which can be used for conversion of waste heat into electrical energy or for refrigeration. Nanostructuring of these materials improves the efficiency of these materials in thermoelectric applications. Method presented in this thesis is simple, cost effective and gives a good yield therefore can be used for large scale production. These nanoscaled cubes of lead chalcogenides are promising for future thermoelectric applications.

References

[1] K. Kordas, G. Toth, P. Moilanen, M. Kumpumaki, J. Vahakangas, A. Uusimaki, R. Vajtai, P.M. Ajayan, *Applied Physics Letters 90 (2007) 123105*.

[2] A. Bar Cohen, A.D. Kraus, S.F. Davidson, *Design and Packaging of Microelectronic Equipment Engineering 105 (6) (1983) 5359.*

[3] L.T. Yeh, *Journal of Electronic Packaging 117 (1996) 333–339.*

[4] Kaveh Aza, *Chip Level Spot Cooling, Chip Scale Review, 17–19, May/ June 2011*.

[5] Raghavendra Nunna, Emmanuel Guilmeau, Franck Gascoin, *Journees de l'Ecole Doctorale Simem (UCCBN) les 24 et 25 avril (2012).*

[6] D.M. Rowe, *International Journal of Innovations in Energy Systems and Power 1 (1) (2006).*

[7] G. Jeffrey Snyder, *The Electrochemical Society Interface (2008)*

[8] Hillal Alam, Seeram Ramakrishnan, *Nano Energy (2013) 2 190-212*

[9] Buyong Wan, Chenguo Hu, Yi Xi, Jing Xu, Xiaoshan He, *Solid State Sciences 12 (2010) 123-127*

[10] Herwin Ahuja, Bao Yang, Thanh N. Tran, *HVAC&R Research 14 (5) (2008) 635–653.*

[11] Giuliano Benenti, Giulio Casati, *Philosophical Transactions of the Royal Society A (2012) 466–481*

[12] Terry M. Tritt, M.A. Subramanian, *MRS Bulletin,Volume 31 march 2006*

[13] Zhi-Gang Chen, Guang Han, LeiYang, Lina Cheng, Jin Zou, *progress in Natural Science: Materials International 2012;22(6):535-549*

[14] H.J. Goldsmid, in: D.M. Rowe (Ed.), *CRC Handbook of Thermoelectrics, CRC Press, 1995.*

[15] C. B. Vining, *"An Inconvenient Truth About Thermoelectrics," Nature Materials* ***8****, 83 (2009).*

[16] T.M. Tritt, H. Bottner, L. Chen, *Thermoelectrics: direct solar thermal energy conversion, MRS Bulletin 33 (2008) 366–368.*

[17] P. Pichanusakorn, P. Bandaru, *Materials Science and Engineering R 67 (19) (2010) 19–63*

[18] M. cutler, J.F. Leavy, R.L. Fitzpatrick, *Physics Review 133 (1964) A1143–A1152*

[19] G.Jeffrey Snyder, S Toberner Eric, *Nature Materials 7 (2008) 105–114.*

[20] D.M. Rowe Ed. *Introduction, CRC Handbook of Thermoelectrics, 1995*.

[21] Alexander A Balandin, Evghenii P Pokatilov, D.L. Nika, *Journal of Nanoelectronics and Optoelectronics 2 (2007) 140–170.*

[22] G.D. Mahan, J.O. Sofo, *Applied Physical Sciences 93 (1996) 7436–7439.*

[23] T.M. Tritt, *Annual Review of Materials Research, in: Encyclopediaof Materials: Science and Technology, Elsevier, 2002. ISBN: 0-08- 043152-6.*

[24] S.B. Riffat, Guoquan Qiu, *Applied Thermal Engineering 24 (14–15) (2004) 1979–1993.*

[25] Jiao Wang, Guilio Casati, Tomaz Prosen, C.H. Lai, *Physical Review E 80 (2009).*

[26] C. Wood, *Materials for thermoelectric energy conversion, Reports on Progress in Physics 51 (1988) 459–539*

[27] P. Vaqueiro, A.V. Powell, *Recent developments in nanostructured materials for high-performance thermoelectrics, Journal of Materials Chemistry 20 (2010) 9577–9584*

[28] G.A. Slack, M. Rowe (Ed.), *CRC Handbook of Thermoelectrics, CRC Press, Boca Raton, FL, 1995*

[29] J. L. Mi, T. J. Zhu, X. B. Zhao, J. Ma, *Nanostructuring and thermoelectric properties of bulk skutterudite compound CoSb3, Journal of Applied Physics 101 (2007) 054314.*

[30] X. Shi, J. Yang, J.R. Salvador, M. Chi, J.Y. Cho, H. Wang et al., *Multiple-filled skutterudites: High thermoelectric figure of merit through separately optimizing electrical and thermal transports, Journal of the American Chemical Society133 (2011) 7837–7846.*

[31] X. Shi, J. Yang, S. Bai, J. Yang, H. Wang, M. Chi, et al., *On the design of high-efficiency thermoelectric clathrates through a systematic cross-substitution of framework elements, Advanced Functional Materials 20 (2010) 755–763.*

[32] Y. Liu, L.M. Wu, L.H. Li, S.W. Du, J.D. Corbett, L. Chen, *The antimony-based type I clathrate compounds Cs(8)Cd(18)Sb(28) and Cs(8)Zn(18)Sb(28), Angewandte Chemie, International Edition 48 (2009) 5305–5308.*

[33] S.K. Bux, J.P. Fleurial, R.B. Kaner, *Nanostructured materials for thermoelectric applications, Chemical Communications 46 (2010) 8311–8324*

[34] J.R. Szczech, J.M. Higgins, S. Jin, *Enhancement of the thermoelectric properties in nanoscale and nanostructured materials, Journal of Materials Chemistry 21 (2011) 4037–4055.*

[35] M.S. Dresselhaus, G. Chen, M.Y. Tang, R.G. Yang, H. Lee, D.Z. Wang, et al., *New directions for low-dimensional thermo- electric materials, Advanced Materials 19 (2007) 1043–1053*

[36] C.J. Vineis, A. Shakouri, A. Majumdar, M.G. Kanatzidis, *Nanostructured thermoelectrics: big efficiency gains from small features, Advanced Materials 22 (2010) 3970–3980.*

[37] Edward Rama Venkatasubramanian, Thomas Siivola, Colpitts, Brooks O Quinn, *Nature 413 (11) (2001) 597–602.*

[38] R. Fletcher, M. Tsaousidou, P.T. Coleridge, Y. Feng, Z.R. Wasilewski, *Physica E 12 (2002) 478–481.*

[39] Alexander Balandin, Kang L Wang, *Journal of Applied Physics 84 (11) (1998) 6149–6153.*

[40] P.S. Nair, K.P. Friz, G. Scholes, *Chem. Commun. 24 (2004) 2084*

[41] H. Du, C. Chen, R. Krishan, T.D. Krauss, J.M. Harbold, F.W. Wise, M.G. Thomas, J. Silcox, *Nano Lett. 2 ,.(2002) 1321*

[42] H. Zogg, K. Kellermann, K. Alchalabi, D. Zimin, *Infrared Phys. Technol. 46 (2004) 155.*

[43] V.V. Shchennikov, S.V. Ovsyannikov, *Solid State Commun. 126 (2003) 373.*

[44] L.D. Hicks, M.S. Dresselhaus, *Effect of quantum-well structures on the thermoelectric figure of merit, Physical Review B 47 (1993) 12727.*

[45] L.D. Hicks, T.C. Harman, M.S. Dresselhaus, *Use of quantum- well superlattices to obtain a high figure of merit from nonconventional thermoelectric materials, Applied Physics Letters 63 (1993) 3230–3232.*

[46] B.Y. Wan, C.G. Hu, B. Feng, Y. Xi, X.S. He, *Mater. Sci. Eng. B 163 (2009) 57.*

[47] Q.Y. Lu, F. Gao, S. Komarneni, *Nanotechnology 17 (2006) 2574*

[48] S.Y. Jing, S.X. Xing, C. Zhao, *Mater. Lett. 62 (2008) 41.*

[49] W.G. Lu, J.Y. Fang, Y. Ding, Z.L. Wang, *J. Phys. Chem. B 109 (2005) 19219.*

[50] H. Tong, Y.J. Zhu, L.X. Yang, L. Li, L. Zhang, Angew. *Chem. Int. Ed. 45 (2006) 7739.*

[51] T. Huang, L. Qi, *Nanotechnology 20 (2009) 025606*

[52] J.Q. Jiao, X. Liu, W. Gao, C.W. Wang, H.J. Feng, X.L. Zhao, L.P. Chen, *Solid State Sci. 11 (2009) 976*

[53] T.C. Harman, P.J. Taylor, M.P. Walsh, B.E. LaForge, *Quantum dot superlattice thermoelectric materials and devices, Science (New York, NY) 297 (2002) 2229–2232.*

[54] K.F. Hsu, S. Loo, F. Guo, W. Chen, J.S. Dyck, C. Uher, et al., *Cubic $AgPb_mSbTe_{m+2}$: bulk thermoelectric materials with high figure of merit, Science (New York, NY) 303 (2004) 818–821.*

[55] J. Androulakis, C.H. Lin, H.J. Kong, C. Uher, C.I.Wu, T. Hogan, et al., *Spinodal decomposition and nucleation and growth as a means to bulk nanostructured*

thermoelectrics: enhanced performance in $Pb_{1-x}Sn_xTe$-PbS, Journal of the American Chemical Society 129 (2007) 9780–9788.

[56] P.F.R. Poudeu, J. D'Angelo, A.D. Downey, J.L. Short, T.P. Hogan, M.G. Kanatzidis, *High thermoelectric figure of merit and nanostructuring in bulk p-type $Na_{1-x}Pb_mSb_yTe_{m+2}$, Angewandte Chemie, International Edition 45 (2006) 3835–3839.*

[57] P.F.P. Poudeu, A. Gueguen, C.I. Wu, T. Hogan,M.G. Kanatzidis *High figure of merit in nanostructured n-type KPb_mSbTe_{m+2} thermoelectric materials, Chemistry of Materials 22 (2010) 1046–1053*

[58] Geochemical Instrumentation and Analysis, Darrell Henry, Nelson Eby, John Goodge, David Mogk

[59] Geochemical Instrumentation and Analysis, Barbara L Dutrow, Louisiana State University ,Christine M. Clark, Eastern Michigan University

[60] Geochemical Instrumentation and Analysis, Susan Swapp, University of Wyoming

[61] Radiological and Environmental management, courtesy of Iowa State University